Available online at BCREC Website: https://bcrec.id

Bulletin of Chemical Reaction Engineering & Catalysis, 14 (3) 2019, 614-624

Research Article

Ruthenium-doped Titania-pillared Clay for The Selective Catalytic Oxidation of Cyclohexene: Influence of Ru Loading

Ahmed Dali[1,2], Ilhem Rekkab-Hammoumraoui[1*], Sanaa El Korso[1], Souheyla Boudjema[1,2], Abderrahim Choukchou-Braham[1]

[1]Laboratory of Catalysis and Synthesis in Organic Chemistry, Faculty of Science at AbouBakr Belkaïd University – P.O.Box 119 - Tlemcen 13000, Algeria.
[2]Faculty of Hydrocarbons, Renewable Energy, Earth Sciences and Universe, Kasdi Merbah University, Ouargla 30000, Algeria.

Received: 22nd April 2019; Revised: 11th July 2019; Accepted: 16th July 2019;
Available online: 30th September 2019; Published regularly: December 2019

Abstract

A series of ruthenium-based catalysts supported on acid-activated montmorillonite (PILC) and interspersed with titanium (Ru/Ti-PILCs) were prepared with various amounts of ruthenium. Their catalytic performances in the selective oxidation of cyclohexene, using tert-butylhydroperoxide (TBHP) as oxidant were checked. The clay structure modification by acid activation and impregnation of transition metals resulted in an enhanced Lewis and Bronsted acidities. The Ru/Ti-PILCs materials were characterized using X-ray diffraction (XRD), surface area and pore volume measurements, surface acidity followed by Fourier transform infrared (FTIR) spectroscopy, chemical analysis, and Scanning Electron Microscopy (SEM). It was found that all catalysts can selectively oxidize cyclohexene through allylic oxidation leading mainly to 2-cyclohexene-1-one (Enone) as the major product, and 2-cyclohexene-1-ol (Enol) as secondary product. With the 5 %Ru/Ti-PILC, it was possible to reach 59 % cyclohexene total conversion, and 87 % selectivity into 2-cyclohexene-1-one and 13 % selectivity into 2-cyclohexene-1-ol.

Keywords: Cyclohexene; Pillared clay; Ruthenium; Selective oxidation; TBHP

How to Cite: Dali, A., Rekkab-Hammoumraoui, I., El Korso, S., Boudjema, S., Choukchou-Braham, A. (2019). Ruthenium-doped Titania-pillared Clay for The Selective Catalytic Oxidation of Cyclohexene: Influence of Ru Loading. *Bulletin of Chemical Reaction Engineering & Catalysis*, 14(3): 614-624 (doi:10.9767/bcrec.14.3.4723.614-624)

Permalink/DOI: https://doi.org/10.9767/bcrec.14.3.4723.614-624

1. Introduction

Clays are polyvalent materials that may be employed in various applications, ranging from ceramics to catalysts. Their wide utilization is mainly due to their properties, such as acidity, surface nature and/or their composition [1,2]. It is worth reminding that in catalysis; only the external surface of the material is active, as large organic molecules cannot dodge in and out layers. Moreover, though non-polar molecules have reduced dimensions, they cannot penetrate into the material due to the hydrophilic character of the layers [3]. In order to obtain thermally stable materials with a greater interlayer distance, cations can be intercalated between the clay layers. These cations act as pillars that help in keeping the silicate layers separated, even in the absence of solvents.

---

* Corresponding Author.
E-mail: ahmed2lcsc@gmail.com

Pillared clays are prepared by exchanging the charge compensating cations, which are normally found in the interfoliary space of the parent clay, with bulky polycations obtained by hydrolysis of chosen metal salts. Upon heating, these polyoxocations undergo structural transformations and are decompose into metal oxyhydroxide clusters, called pillars, which maintain the clay layers apart thus precluding their collapse. The resulting material is stable, with acidic character. It also presents a porous structure generated by the intercalation of the interfoliary space [4-9]. A variety of oxides, such as: Al_2O_3 [10], ZrO_2 [11], TiO_2 [11], Fe_2O_3 [12], SnO_2 and mixed oxides, like SiO_2-Fe_2O_3, SiO_2-TiO_2 [13], TiO_2-ZrO_2 [14], and Fe_2O_3-TiO_2 [15], have been successfully employed to get pillared clays. The pillared clays are generally known to be stable up to a temperature range of 500-700 °C.

In addition to supporting the layers, the metal oxide pillars contribute to the acidity of the material. This involves the generation of structures with both Bronsted and Lewis acidities, which may influence the composition of the products obtained in organic catalytic reactions. The acidity of the obtained material is greater than that of the initial clay or parent clay [16]. The increase in the clay's acidy is ascribed to two factors: first, the larger specific surface area of the clay, as compared to that of non-pillared clay and, second, the appearance of new acid sites on pillars and in the sites existing between the clay layers and pillars. The Bronsted acidity is associated with the liberation of protons during the dehydroxylation of the pillars and the clay sheets, while the Lewis acidity is attributed to the metal oxide pillars. The strength and number of sites of both acids are directly related to the nature of clays and pillars [17].

The allylic oxidation of alkenes is an important and useful reaction in many industries [18]. The allylic oxidation of cyclohexene has been the subject of many papers in recent years [19- 25] and many catalysts, such as: nitrogen-doped carbon nanotubes (N-CNTs) [26], VO_2-SiO_2 [27], mixed oxides (Ru/Co/Ce) [28], zeolite-Y entrapped transition metal complexes [29], manganese porphyrins [30], PdO/SBA-15 [31], Fe-MIL-101 and Metal-organic frameworks MIL-101(Cr) [32], have been studied.

Up to now, the cases of catalytic allylic oxidation of cyclohexene in the presence of clays or pillared clays have been uncommon and, to the best of our knowledge, RuO_2 has not been used in the cyclohexene oxidation reactions, although Ru complexes have been extensively used in a large number of epoxidation reactions, among which are the epoxidation of propene, octene, cyclohexene, cyclooctene, styrene, etc. [33,34]. Thus, and for the first time, we considered it interesting to evaluate the supported-RuO_2 catalytic oxidation of cyclohexene.

The fact that PILCs present an acidic character and have a porous structure makes them interesting and efficient supports for catalytic applications. Earlier, our group has performed some studies on the preparation, characterization of ruthenium impregnate H-Montmorillonite (H-Mont) and Ti-pillared clay (Ti-PILC) for cyclohexene oxidation with tert-butylhydroperoxide (TBHP) as oxidant [35]. In continuation of these works, we have prepared and characterized 1 - 3 wt% Ru/Ti-PILC to be tested in the oxidation reaction. The final aim of this complementary study is to gather all results obtained by our group in order to highlight the mechanism of cyclohexene oxidation.

2. Materials and Method

2.1 Ruthenium Supported Ti-pillared Montmorillonite Synthesis

Ti-PILC was prepared following the procedure proposed by Bineesh *et al.* [36] and described in our early work [35]. The used raw montmorillonite comes from the town of Maghnia (Western Algeria). Its basal spacing is 1.44 nm and its S_{BET} is 195 m^2/g. Its cation exchange capacity is 0.34 meq per/g. The Ti-PILC supported Ru catalysts were prepared by the conventional wet impregnation process, in acetone suspensions, in order to obtain materials containing 1 to 3 wt% of ruthenium. $Ru(acac)_3$ was used as the precursor salt. The obtained solids were dried for 72 h at 60 °C, and then calcined under atmospheric air for 4 h at 240 °C. This was performed with the heating rate of 3 $°C.min^{-1}$ [37].

2.2 Measurements

The amount of Ru in the prepared catalysts was determined by means of a Perkin Elmer AA300 Flame Atomic Absorption Spectrophotometer. The pre-processing was carried out by acid dissolution. The X-ray powder diffraction (XRD) patterns were obtained using a Rigaku D/max 2500 powder X-ray diffractometer with a Cu Kα radiation (λ =1.541874 Å) in the range 2θ = 2–70°, with a step of 0.02° and an acquisition time of 1 s.

The Micromeritics Quantachrome NOVA 1000 instrument analyzer was used to determine the adsorption–desorption isotherms at

77 K. Prior to measurements, the samples were outgassed at 250 °C for 3 h. The specific areas were estimated according to the Brunauer-Emmett-Teller (BET) equation.

The FTIR spectra of the solid samples were recorded using an Agilent Technologies Cary 640 spectrometer. FTIR analysis of chemisorbed pyridine was conducted on an Agilent Technologies Cary 640 spectrometer equipped with an ATR accessory in order to determine the acidic properties of the samples. Measurements were carried out following the procedure described in a previous work [38]. SEM Micrographies were collected on a Hitachi-TM.1000 at a 150 KV acceleration voltage, coupled with EDX analysis (energy-dispersive X-rays).

2.3 Catalytic Evaluation of Solids

The oxidation reaction of cyclohexene with tert-butylhydroperoxide TBHP (70 wt.% in H_2O, Aldrich) as oxidant was carried out in a 100 mL three neck glass round bottom flask fitted with a water condenser, magnetic stirrer and thermometer. Initially, 5.5 mL (38.45 mmol) of oxidant were mixed to 25 mL of heptane (solvent) and stirred for 24 h in a closed Erlenmeyer flask. This operation was performed in order to achieve a phase transfer of TBHP from water to organic phase. The organic phase was then isolated from the aqueous one. An iodometric titration was performed to control the concentration of the remaining TBHP in the aqueous phase (<10 % of initial TBHP). A glass reactor was then charged with the organic phase (TBHP-heptane mixture), 29 mmol (3 mL) of cyclohexene and 0.1 g of catalyst, heated under vigorous stirring at 70 °C during 6 h. The reaction products were analyzed by gas chromatography (GC), using a GC-6500-YL-Instrument system equipped with an Agile HP-FFAP capillary column and a flame ionization detector (FID). The remaining TBHP was analyzed at the end of the reaction (after 6 h), by iodometric titration. The conversion, the selectivity of products and the turnover frequency were calculated using the following equations:

$$Conversion\,(\%) = \frac{[Cyclohexene]_0 - [Cyclohexene]_t}{[Cyclohexene]_0} \times 100 \qquad (1)$$

$$Selectivity\,(\%) = \frac{(Moles\ of\ individual\ product)}{(Moles\ of\ total\ products)} \times 100 \qquad (2)$$

$$TOF\,(h^{-1}) = \frac{(Moles\ of\ products)}{(Moles\ of\ catalysts) \times (time)} \qquad (3)$$

3. Results and Discussion

3.1 Characterization of Samples

The XRD patterns of (x = 1-5 wt %) Ru/Ti-PILC are shown in Figure 1. The two-dimensional diffractions hk of PILCs located at 19.8° and 35.8° are characteristic of montmorillonite (for Ti-PILC d_{001} is observed at 2θ = 3.3° related to the basal spacing of 2.67 nm) [35]. The first diffraction is the sum of the indexes hk of (02) and (11), while the last one is the sum of the indexes hk (13) and (20). Moreover, the reflections at 2θ = 25°, 38°, 48° and 53° are observed for anatase-titanium (JCPDS: 21-

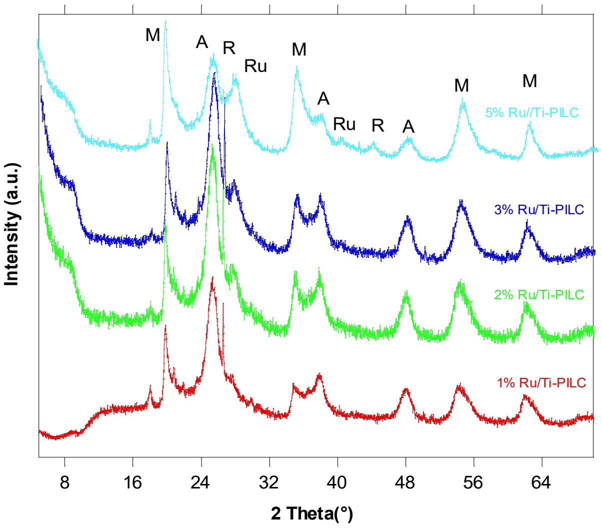

Figure 1. XRD patterns of the supported materials (M: Montmorillonite; A: Anatase; R: Rutile; Ru: RuO_2)

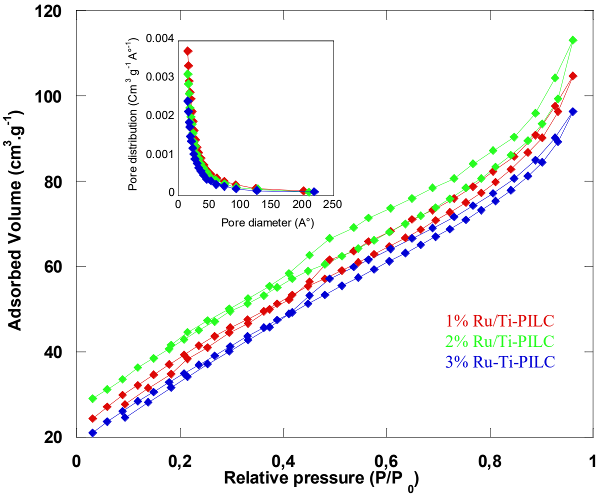

Figure 2. N_2 adsorption–desorption isotherms and BJH-pore size distribution of the supported samples

1272) [39]. The appearance of peaks at 2θ = 28° and 35° suggests the presence of ruthenium oxide in our materials (JCPDS: 40-1290). With the increase of Ru content, the anatase peaks intensities gradually decrease and the rutile appears at 2θ = 27°, 36° and 41° (JCPDS: 21-1276), even when the Ru content reaches 3 %.

The N_2 adsorption-desorption isotherms and pore size distributions of Ti-PILC and the supported catalysts are displayed in Figure 2. The isotherms data of 1, 2 and 3 %Ru Ti-PILC catalysts are type VI isotherms (Figure 2), with an H4 type hysteresis loop following the IUPAC classification [40]. This type of isotherms is characteristic of the presence of mesopores. The hysteresis indicates the presence of micropores as well. Insert of the Figure 2 shows that the BJH pore size distribution of all samples presents a unimodal and narrow peak, centred at 15 Å. However, an increase in the ruthenium oxide loading onto the Ti-PILC support (S_{BET}= 278 $m^2.g^{-1}$) [35] decreased the surface area, probably because of pore blockade resulting from their progressive filling with ruthenium species (Table 1) [41- 43].

Figure 3 shows the FTIR spectra of 1, 2, and 3 %Ru/Ti-PILC materials. The FTIR spectrum of materials exhibits two bands at 3642 and 3448 cm^{-1} in the –OH stretching region. These bands are attributed to the clay structural hydroxyl groups and water molecules in the interlayers [42,44].

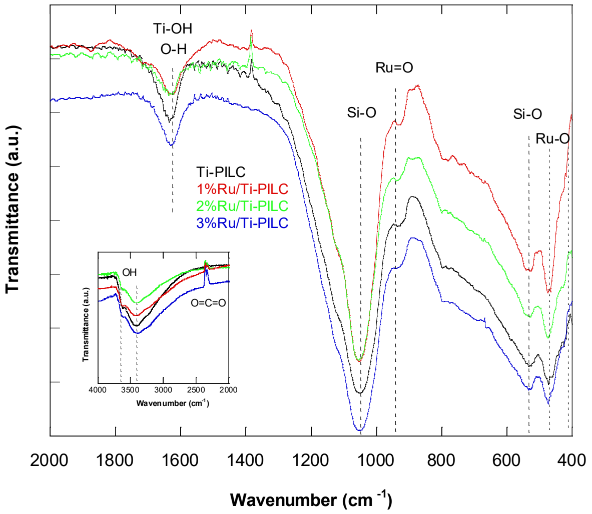

Figure 3. FTIR spectra of the supported materials

The band around 1600 cm^{-1} is attributed to the bending vibrations of water and Ti–OH [45]. The strong band around 1040 cm^{-1} is characteristic of the asymmetric stretching vibrations of tetrahedral SiO_2 [46]. The band at 524 cm^{-1} can be ascribed to the Si–O bending vibrations. On the other hand, the absorptions observed at 442, 430, 428 cm^{-1} [47], and also around 668 cm^{-1} [48] represent the Ru–O groups. The peak detected at 980 cm^{-1} correspond to the Ru=O peak [49,50]. The bands at 1457, 1540, and 2903 cm^{-1} were observed for ruthenium supported catalysts. They can be assigned to the presence of –C=C, –C=O, and –C–H groups, respectively. However, these bands were not observed in purified clay or pillared clay, which suggests that the acetylacetonate salt was not completely removed from the supported samples after calcinations.

The infrared (IR) spectroscopy in the region from 1400 to 1600 cm^{-1} was carefully checked, in order to study the pyridine adsorption on the clay surface in order to better determine the acidity of the clay. The band at 1450 cm^{-1} can be attributed to Lewis acid sites (Lpy) [51] and the band at 1540 cm^{-1} is due to Bronsted acid sites (Bpy) [52]. The concentrations of Lewis and Bronsted acid sites were calculated from the integrated intensities of the Bpy and Lpy bands (1450 and 1540 cm^{-1}) and the values of the molar absorption coefficients of these bands, equal to 1.13 and 1.28 cm μmol^{-1}, respectively, as previously determined by Guisnet et al. [53] while studying the sorption of given amounts of pyridine on H-mordenite (containing only Bronsted sites) and on alumina (containing only Lewis sites). The results obtained are shown in Table 2. They indicate that the number of Lewis acid sites is distinctly higher than that of Bronsted acid sites for Ti-PILC. Data from the literature on Ti-PILC indicate the presence of both Lewis and Bronsted acidities, with the Lewis acid being more dominant [54]. In general, the pillaring of clay causes a considerable increase in acidity. This in-

Table 1. Textural properties and metal content of the samples

	1 %Ru/Ti-PILC	2 %Ru/Ti-PILC	3 %Ru/Ti-PILC
Ru $_{loading}$ (%)	0.95	1.87	2.86
S_{BET} ($m^2.g^{-1}$)	248	238	226
V_p ($cm^3.g^{-1}$)	0.30	0.31	0.35
d_p (Å)	15	15	19

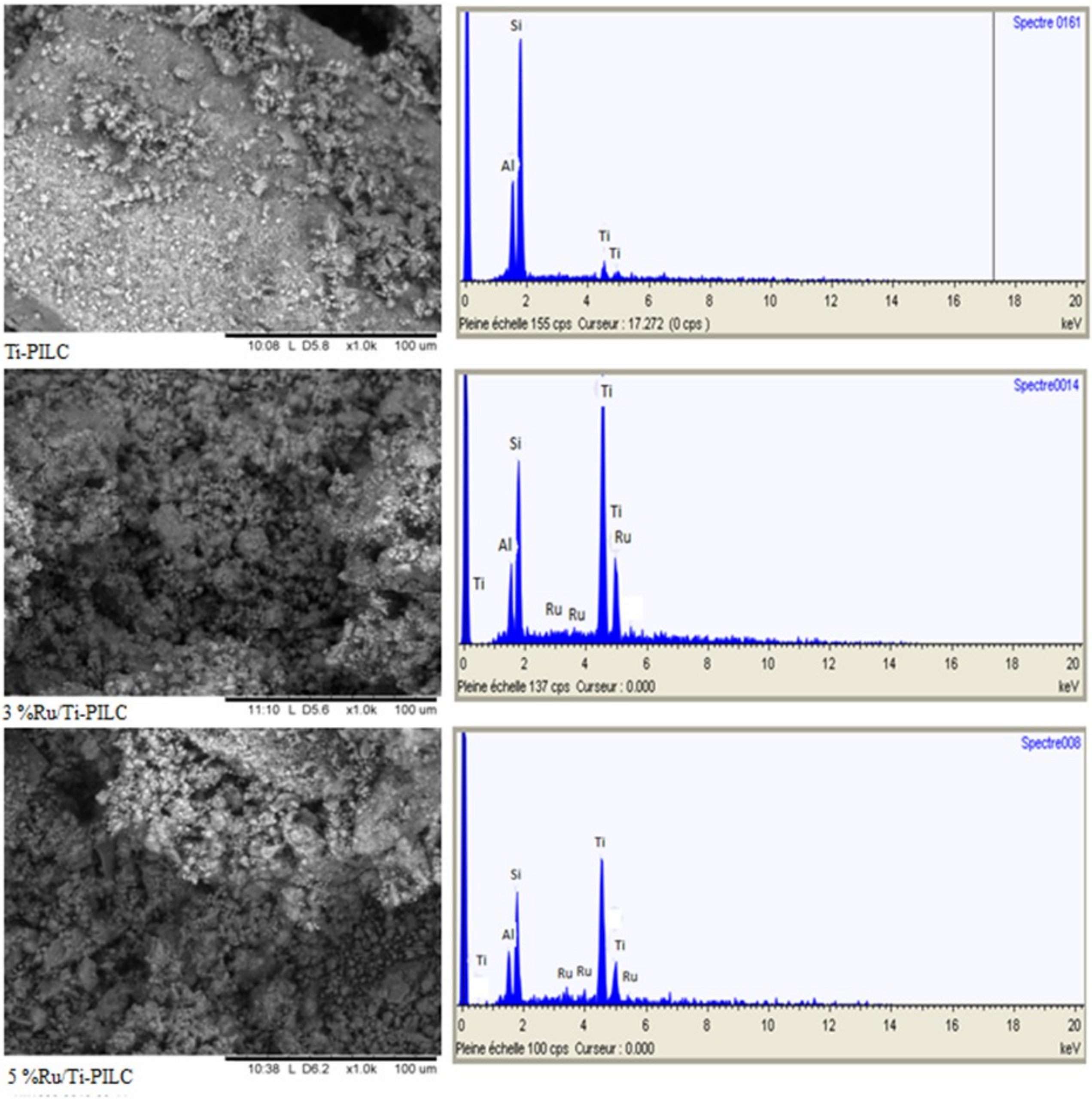

Figure 4. SEM micrographs and EDX analysis of Ti-PILC, 3 %Ru/Ti-PILC and 5 %Ru/Ti-PILC materials

Table 2. Lewis and Bronsted acidity (µmol.g^{-1}) of Ti-PILC and its supported Ru materials upon adsorption of pyridine

Catalyst	Lewis acid sites (Lpy) µmol.g^{-1}	Bronsted acid sites (Bpy) µmol.g^{-1}	Lpy +Bpy µmol.g^{-1}	[Lpy]/[Bpy]
Ti-PILC	260	87	347	2.98
1 %Ru/Ti-PILC	186	93	279	2.00
3 %Ru/Ti-PILC	300	105	405	2.85
5 %Ru/Ti-PILC	434	116	550	3.74

elsewhere [35]. The best catalytic performance previously reported is 5 %Ru/Ti-PILC, which presents a conversion of 59 % with 89 % and 11 % selectivities for 2-cyclohexene-1-one 2- and cyclohexene-1-ol, respectively. In comparison to other reports presented in the literatures (Tables 4 and 5), it can be established that this catalyst 5 %Ru/Ti-PILC is the most interesting one. It is worth mentioning that incorporating TiO_2 into clay could further enhance the catalyst activity and products selectivity. Qadir *et al.* [58] indicated that TiO_2 was able to boost the cyclohexene oxidation to yield cyclohexen-1-one and cyclohexen-1-ol. Layered clays have been extensively used as acid catalysts and as supports alike. IR spectroscopy has been utilized to prove that the metal oxide pillars are responsible for the Lewis acidity; the Bronsted acid sites are located on the clay sheets [59]. As a conclusion, one may therefore say that Bronsted and Lewis acid sites in PILC are effective in catalysing the oxidation of cyclohexene, as this can be explained by the Mars and van Krevelen mechanism [59]. Additionally, using TBHP as oxidant under the conditions of an acid catalyst enhances the allylic oxidation pathway, while decreasing the epoxidation [60]. Several mechanisms of cyclohexene oxidation are much debated in the literature and many intermediate complexes are suggested [27,61-63].

Based on our experimental observations and literature reports, a mechanism of cyclohexene oxidation, catalysed by the materials Ru/Ti-PILC developed in the present article, is described in Scheme 1, according to which the initial complex combination of metal catalyst and tert-butyl hydroperoxide makes peroxidic oxygen more electrophilic and hence more labile to attack by an olefinic double bond. Then

Table 5. A summary of the catalysts used in the literature for the oxidation of cyclohexene

Catalyst	Substrate	Conversion (%)	Selectivity (%)					Ref.
			Enol	Enone	Epoxide	Diol	One	
Ti-PILC	Cyclohexene, TBHP as oxidant, heptane as solvent, 70 °C, 6 h, 0.1 g catalyst	26	89	11	0	0	0	[35]
5 %Ru/Ti-PILC	Cyclohexene, TBHP as oxidant, heptane as solvent, 70 °C, 6 h,0.1 g catalyst	59	13	87	0	0	0	[35]
6 %V/Fe-Mont	Cyclohexene, TBHP as oxidant, heptane as solvent, 70 °C, 6 h, 0.1 g catalyst	87	3	7	67	7	16	[12]
15 %V/Cr-AAC	Cyclohexene, TBHP as oxidant, heptane as solvent, 70 °C, 6 h, 0.05 g catalyst	38.3	2	4.4	65	10.3	18.3	[64]
Au/monolith	Cyclohexene, TBHP as oxidant, acetonitrile as solvent, 30 °C, 6 h, 0.05 g catalyst	18.3	16	81.5	2.5	0	0	[56]
Ru/CeO_2	Cyclohexene, TBHP as oxidant, 1,2-dichloroethane as solvent, 60 °C,12 h, 0.005 g catalyst	38.1	40.5	49.6	5.7	0	4.2	[65]
$RuC1_2(4\text{-Mepy})_4$	Cyclohexene, CHP (cumenehydroperoxide) as oxidant, THF as solvent, 50 °C,5 h, 2.9 10^{-5} mole catalyst	-	48.7	51.7	0	0	0	[66]
Co_3O_4	Cyclohexene, TBHP as oxidant, heptane as solvent, 70 °C, 6 h,0.1 g catalyst	78	43	41	0	0	16	[67]

crease is due to the intercalation and presence of metal oxide pillars [54].

The addition of ruthenium oxide to Ti-PILC increased more significantly the number of Lewis acid sites, comparatively to Bronsted acid sites. Furthermore, a strong increase in the total acidity was observed when moving from the starting Ti-PILC to the supported Ti-pillared materials. Based on the infrared spectra of adsorbed pyridine, Sorlino *et al.* [55] concluded that ruthenium oxide ions display a rather strong Lewis acidity on the face of RuO$_2$. Bronsted acids involve OH groups.

The ratio of the numbers of Lewis vs Bronsted sites is also presented in Table 2. It can be seen that this ratio increases gradually as the ruthenium loading rises. This may be due to the weak interaction of RuO$_2$ with the support, which facilitates the access of the single pair of free electrons from ruthenium oxide to the clay surface. The studied samples can thus be ordered with respect to the number of acid sites as follows: 5 %Ru/Ti-PILC > 3 %Ru/Ti-PILC > 1 %Ru/Ti-PILC > Ti-PILC.

The SEM micrographs coupled with EDX analysis are presented in Figure 4. Ti-PILC micrograph shows large particles with smooth surfaces coexisting with fine grains probably TiO$_2$. Whereas, micrographs of the supported Ti-pillared materials shows a homogeneous distribution of small grains covering completely the clay surface [56]. EDX microanalysis shows the structural elements of clay, namely silicon and aluminum. The presence of TiO$_2$ indicated the existence of pillars in the clay. The ruthenium loadings of catalysts 3 %Ru/Ti-PILC and 5 %Ru/Ti-PILC were determined to 2.79 wt.% Ru and 4.18 wt.% Ru, respectively (see Table 3).

Table 3. EDX analysis results of Ti-PILC, 3%Ru/Ti-PILC, and 5%Ru/Ti-PILC materials

Component	Ti-PILC (wt.%)	3 %Ru/Ti-PILC (wt.%)	5 %Ru/Ti-PILC (wt.%)
SiO$_2$	28.30	25.75	22.44
Al$_2$O$_3$	12.82	11.91	14.37
TiO$_2$	58.88	59.55	58.99
RuO$_2$	0	2.79	4.20

3.2 Catalytic Oxidation of Cyclohexene

Cyclohexene oxidation with tert-butyl hydroperoxide (TBHP) over the studied materials gives several products, following two pathways: (i) the oxidation at the allylic position yielding 2-cyclohexene-1-ol (Enol), 2-cyclohexene-1-one (Enone), cyclohexanol (Ol), cyclohexanone (One), and (ii) the oxidation of the double bound, resulting in cyclohexane oxide (Epoxide) and cyclohexane diols (Diol). Table 3 sums up all the catalytic results of cyclohexene oxidation over the catalysts. No oxidation product was obtained in the absence of catalysts [32].

In all catalytic experiments, it was found that the cyclohexene conversion increases with the ruthenium content from 18 % with a turnover frequency (TOF) of 88 h^{-1} over 1 %Ru/Ti-PILC to 44 % and a TOF of 72 h^{-1} over 3%Ru/Ti-PILC. The oxidation reaction preferentially happened within the activated allylic C–H bond, which led to the selective products 2-cyclohexene-1-one and 2-cyclohexene-1-ol. In fact, the selectivity for 2-cyclohexene-1-ol decreased from 61 % to 39 %, and the selectivity for 2-cyclohexene-1-one increased from 39 % to 60 %. This may be due to the fact that Ru/Ti-PILC, which has strong Lewis acid sites (Table 2), favors the formation of Enone [57].

The oxidation of cyclohexene with TBHP in the presence of 5 %Ru/Ti-PILC was studied

Table 4. Cyclohexene oxidation using different supported catalysts

Catalyst	Activity		Selectivity (%)						TBHP Consumption (%)
	Conversion (%)	TOF (h^{-1})	Enol	Enone	Epoxide	Diol	One	Ol	
Blank	0	/	0	0	0	0	0	0	0
1 %Ru/Ti-PILC	18	88	61	39	0	0	0	0	43
2 %Ru/Ti-PILC	42	103	42	58	0	0	0	0	44
3 %Ru/Ti-PILC	44	72	39	60	0	0	0	0	40
5 %Ru/Ti-PILC	59	58	13	87	0	0	0	0	73

C_6H_{12} = 3 mL; TBHP = 5.5 mL; solvent = 25 mL; catalyst = 0.1 g; t = 6 h; T = 70 °C;
TOF = mole of converted cyclohexene per unit time per mole of dispersed ruthenium.

the anion ^{t}BuO-, resulting from the reaction that occurs in parallel to the complex attacks on the C6 ring, leading to the formation of an unsaturated alcohol which undergoes a new oxidation reaction that gives cyclohexenone. The radical mechanism happens especially in the presence of H_2O_2 or O_2 as oxidant. Both of these reagents are known to generate free radicals [68-70].

4. Conclusions

The goal of the present work was to develop clay-based materials to be used as green catalysts in the reaction of cyclohexene oxidation. Both Lewis and Bronsted acid sites were evidenced in these catalysts, as determined by the FT-IR analysis. It was shown herein that the acid sites guided the reaction towards allylic oxidation. The addition of ruthenium to the titanium-pillared clay enhanced the activity of pillared clay significantly. In the presence of 5 %Ru/Ti-PILC catalyst, cyclohexene was converted in 59 %, to primarily 2-cyclohexen-1-one (selectivity = 87 %) and to 2-cyclohexen-1-ol as a by-product, in the presence of TBHP, at the temperature of 70 °C. The oxidation of cyclohexene was really heterogeneous and no ruthenium leaching was observed.

Conflicts of interest

There are no conflicts to declare.

Acknowledgements

The authors gratefully acknowledge the financial support provided by the General Direction for Scientific and Technological Research (DGRST) as well as the Thematic Research Agency for Science and Technology (ATRST), for the project PNR-8-U13-880. The authors also thank Pr. S. Bedrane from LCSCO for her valuable help in revising the manuscript.

References

[1] Murray, H.H. (2000). Traditional and new applications for kaolin, smectite, and palygorskite: a general overview. *Applied Clay Science*, 17: 207-221.

[2] Vaccari, A. (1999). Clays and catalysis: a promising future. *Applied Clay Science*, 14: 161-98.

[3] Dal Bosco, S.M., Jimenez, R.S., Vignado, C., Fontana, J., Geraldo, B., Figueiredo, F.C.A., Mandelli, D., Carvalho, W.A. (2006). Removal of Mn(II) and Cd(II) from wastewaters by natural and modified clays. *Adsorption*, 12: 133-146.

[4] Gil, A., Gandia, L.M., Vicente M.A. (2000). Recent Advances in the Synthesis and Catalytic Applications of Pillared Clays. *Catalysis Review*, 42: 145-212.

[5] Vaccari, A. (1998). Preparation and catalytic properties of cationic and anionic clays. *Catalysis Today*, 41: 53 -71.

[6] Vaughan, D.E.W. (1988). Pillared clays - A historical perspective. *Catalysis Today*, 2: 187-98.

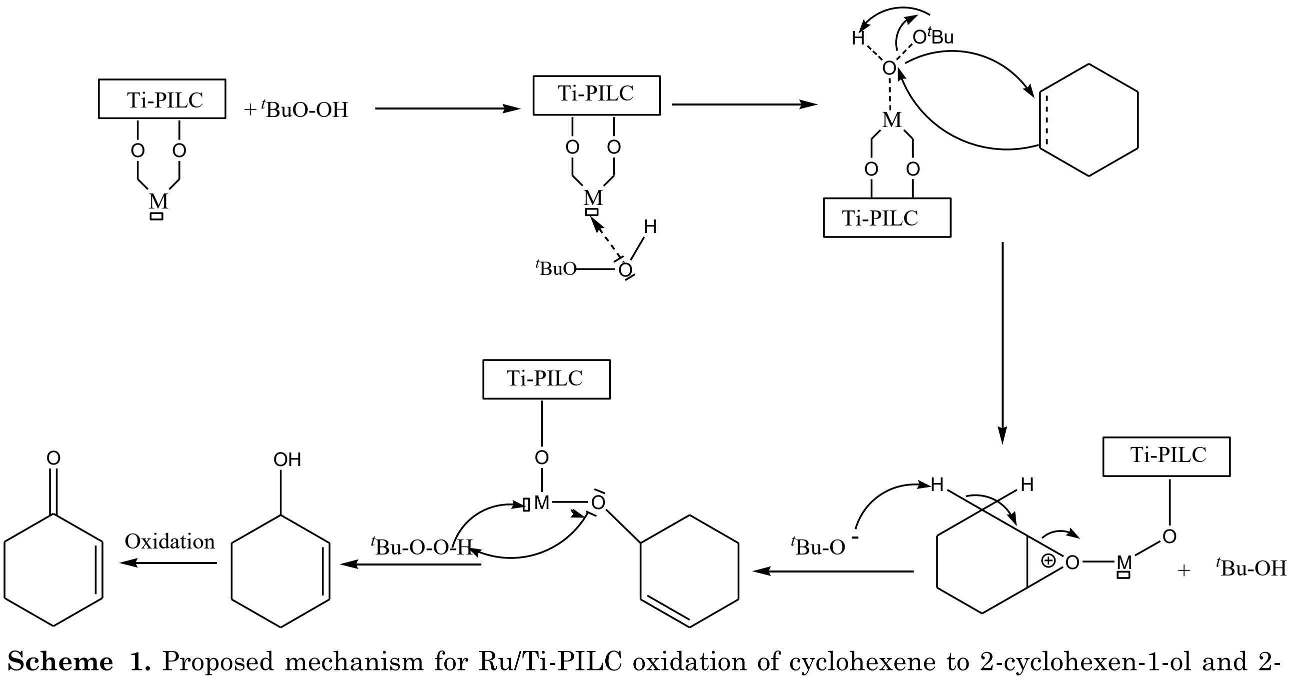

Scheme 1. Proposed mechanism for Ru/Ti-PILC oxidation of cyclohexene to 2-cyclohexen-1-ol and 2-cyclohexen-1-one

[7] Figueras, F. (1988). Pillared Clays as Catalysts. *Catalysis Review*, 30: 457-499.

[8] Lambert, J.F., Poncelet, G. (1997). Acidity in pillared clays: origin and catalytic manifestations. *Topics in Catalysis*, 4: 43-56.

[9] Pinnavaia, T.J. (1983). Intercaled Clay Catalysts. *Science*, 220: 365-371.

[10] Basoglu, F.T., Balci, S. (2016). Catalytic properties and activity of copper and silver containing Al-pillared bentonite for CO oxidation. *Journal of Molecular Structure*, 1106: 382-389.

[11] Bineesh, K.V., Kim, D.K., Cho, H.J., Park D.W. (2010). Synthesis of metal-oxide pillared montmorillonite clay for the selective catalytic oxidation of H_2S. *Journal of Industrial and Engineering Chemistry*, 16: 593-597.

[12] Brahimi, S., Boudjema, S., Rekkab, I., Choukchou-Braham, A., Bachir, R. (2015). Synthesis and Catalytic Activity of Vanadia-Doped Iron-Pillared Clays for Cyclohexene Epoxidation. *Research Journal of Pharmaceutical, Biological and Chemical Sci*ences, 6: 63-76.

[13] Chmielarz, L., Kowalczyk, A., Wojciechowska, M., Boroń, P., Dudek, B., Michalik, M. (2014). Montmorillonite intercalated with SiO_2, SiO_2-Al_2O_3 or SiO_2-TiO_2 pillars by surfactant-directed method as catalytic supports for DeNOx process. *Chemical Paper*, 68: 1219–1227.

[14] Bahranowski, K., Włodarczyk, W., Wisła-Walsh, E., Gaweł, A., Matusik, J., Klimek, A., Gil, B., Michalik-Zym, A., Dula, R., Socha, R.P., Serwicka, E.M. (2015). [Ti,Zr]-pillared montmorillonite – A new quality with respect to Ti- and Zr-pillared clays. *Microporous Mesoporous Materials*, 202: 155-164.

[15] Tomul, F., Basoglu, F.T., Canbay, H. (2016). Determination of adsorptive and catalytic properties of copper, silver and iron contain titanium-pillared bentonite for the removal bisphenol A from aqueous solution. *Applied Surface Science*, 360: 579-593.

[16] Occelli, M.L., Tindwa, R.M. (1983). Physicochemical properties of montmorilloniteinterlayed with cationic oxyaluminumpilllars. *Clays and Clay Minerals*, 31: 22-28.

[17] Zhao, D., Yang, Y., Guo, X. (1995). Synthesis and characterization of hydroxy-CrAI pillared clays. *Zeolites*, 15: 58-66.

[18] Jiang, D., Mallat, T., Meier, D.M., Urakawa, A., Baiker, A. (2010). Copper metal–organic framework: Structure and activity in the allylic oxidation of cyclohexene with molecular oxygen. *Journal of Catalysis*, 270: 26-33.

[19] Parra da Silva, F., Gonçalves, R.V., Rossi, L.M. (2017). Magnetically recoverable copper oxide catalysts for aerobic allylic oxidation of cyclohexene. *Journal of Molecular Catalysis A: Chemical*, 426: 534–541.

[20] Rekkab-Hammoumraoui, I., Khaldi, I., Choukchou-Braham, A., Bachir, R. (2013). TiO_2–SiO_2 mixed oxides: Xerogel catalyst for the Selective Epoxidation of cyclohexene. *Research Journal of Pharmaceutical, Biological and Chemical Sciences*, 4: 935-946.

[21] Driss, L., Choukchou-Braham, A., Kappenstein, C., Pirault-Roy, L. (2012). Synthesis, characterization and activity in cyclohexene epoxidation of V_2O_5–TiO_2 anatasexerogel. *Journal of Sol-Gel Science and Technology*, 64: 637-642.

[22] Ameur, N., Bedrane, S., Bachir, R., Choukchou-Braham., A. (2013). Influence of nanoparticles oxidation state in gold based catalysts on the product selectivity in liquid phase oxidation of cyclohexene. *Journal of Molecular Catalysis A: Chemical*, 374-375: 1-6.

[23] EL-Korso, S., Rekkab, I., Choukchou-Braham, A., Bedrane, S., Pirault-Roy, L.,Kappenstein, C. (2012). Synthesis of vanadium oxides 5 wt.%VO_2–M_xO_y by sol–gel process and application in cyclohexene epoxidation. *Bulletin of Material Science*, 35: 1187-1194.

[24] El-Korso, S., Bedrane, S., Choukchou-Braham, A., Bachir, R. (2015). The effect of redox properties of ceria-supported vanadium oxides in liquid phase cyclohexene oxidation. *RSC Advances*, 5: 63382-63392.

[25] Hakat, Y., Kotbagi, T.V., Bakker, M.G. (2016). Silver supported on hierarchically porous SiO_2 and Co_3O_4 monoliths: Efficient heterogeneous catalyst for oxidation of cyclohexene. *Journal of Molecular Catalysis A: Chemical*, 411: 61-71.

[26] Cao, Y., Yu, H., Wang, H., Peng, F. (2017). Solvent effect on the allylic oxidation of cyclohexene catalyzed by nitrogen doped carbon nanotubes. *Catalysis Communications*, 88: 99-103.

[27] El-Korso, S., Khaldi, I., Bedrane, S., Choukchou-Braham, A., Thibault-Starzyk, F., Bachir, R. (2014). Liquid phase cyclohexene oxidation over vanadia based catalysts with tert-butyl hydroperoxide: Epoxidation versus allylic oxidation. *Journal of Molecular Catalysis A: Chemical*, 394: 89-96.

[28] Ghiaci, M., Aghabarari, B., Botelho do Rego, A.M., Ferraria, A.M., Habibollahi, S. (2011). Efficient allylic oxidation of cyclohexene catalyzed by trimetallic hybrid nano-mixed oxide (Ru/Co/Ce). *Applied Catalysis A: General*, 393: 225-230.

[29] Godhani, D.R., Nakum, H.D., Parmar, D.K., Mehta, J.P., Desai, N.C. (2016). Tuning of the

reaction parameters to optimize allylic oxidation of cyclohexene catalyzed by zeolite-Y entrapped transition metal complexes. *Journal of Molecular Catalysis A: Chemical*, 415: 37-55.

[30] Rutkowska-Zbik, D., Witko, M., Serwicka, E.M. (2011). Allylic oxidation of cyclohexene catalyzed by manganese porphyrins: DFT studies. *Catalysis Today*,169: 10-15.

[31] Ganji, S., Bukya, P., Vakati, V., Rao, K.S.R., Burri, D.R. (2013). Highly efficient and expeditious PdO/SBA-15 catalysts for allylic oxidation of cyclohexene to cyclohexenone. *Catalysis Science & Technology*, 3: 409-414.

[32] Skobelev, I.Y., Sorokin, A.B., Kovalenko, K.A., Fedin, V.P., Kholdeeva, O.A. (2013). Solvent-free allylic oxidation of alkenes with O_2 mediated by Fe- and Cr-MIL-101. *Journal of Catalysis*, 298:61-69.

[33] Chatterjee, D., Basak, S., Mitra, A., Sengupta, A., Le Bras, J., Muzart, J. (2005). Synthesis and catalytic activity of a novel ruthenium(III) complex containing a sugar-based ligand. *Catalysis Communications*, 6: 459-461.

[34] de Souza, V.R., Nunes, G.S., Rocha, R.C., Toma, H.E. (2003). Spectroscopy, electrochemistry and catalytic properties of ruthenium II complexes containing the tetradentate Schiff base ligand N,N′-bis(7-methyl-2-pyridylmethylene)-1,3-diiminopropane. *Inorganica Chimica Acta*, 348: 50-56.

[35] Dali, A., Rekkab-Hammoumraoui, I., Choukchou-Braham, A., Bachir, R. (2015). Allylic oxidation of cyclohexene over ruthenium-doped titanium-pillared clay. *RSC Advances*, 5: 29167-29178.

[36] Bineesh, K.V., Kim, D.K., Kim, M.I.L., Park, D.W. (2011). Selective catalytic oxidation of H2S over V_2O_5 supported on TiO_2-pillared clay catalysts in the presence of water and ammonia. *Applied Clay Science*, 53: 204-211.

[37] Bernas, A., Kumar, N., Laukkanen, P., Vayrynen, J., Salmi, T., Murzin, D.Y. (2004). Influence of ruthenium precursor on catalytic activity of Ru/Al_2O_3 catalyst in selective isomerization of linoleic acid to cis-9,trans-11- and trans-10,cis-12-conjugated linoleic acid. *Applied Catalysis A: General*, 267: 121-33.

[38] Rekkab-Hammoumraoui, I., Choukchou-Braham, A., Pirault-Roy, L., Kappenstein, C. (2011). Catalytic oxidation of cyclohexane to cyclohexanone and cyclohexanol by tert-butyl hydroperoxide over Pt/oxide catalysts. *Bulletin of Material Science*, 34: 1127-1135.

[39] Romero, A., Dodorado, F., Asencio, I., Garcia, P.B., Valverde, J.L. (2006). Ti-pillared clays: synthesis and general characterization. *Clays and Clay Minerals*, 54:737-747.

[40] Brunauer, S., Deming, L.S., Deming, W.E., Teller, E. (1940). Theory of the van der Waals adsorption of gases. *Journal of American Chemical Society*, 62: 1723-1732.

[41] Kim, M., Lee, G., Kim, D.W., Kang, D.H., Park, D.W. (2014). Production of elemental sulfur and ammonium thiosulfate by H_2S oxidation over Nb_2O_5 supported on Fe-pillared clay. *Korean Journal of Chemical Engineering*, 31: 2162-2169.

[42] Bineesh, K.V., Kim, D.K., Kim, D.W., Cho, H.J., Park, D.W. (2010). Selective catalytic oxidation of H_2S to elemental sulfur over V_2O_5/Zr-pillared montmorillonite clay. *Energy & Environmental Science*, 3: 302-310.

[43] Sahel, K., Bouhent, M., Belkhadem, F., Ferchichi, M., Dappozze, F., Guillard, C., Figueras, F. (2014). Photocatalytic degradation of anionic and cationic dyes over TiO_2 P25, and Ti-pillared clays and Ag-doped Ti-pillared clays. *Applied Clay Science*, 95: 205-210.

[44] Binitha, N.N., Sugunan, S. (2006). Preparation, characterization and catalytic activity of titania pillared montmorillonite clays. *Microporous and Mesoporous Materials*, 93:,82-89.

[45] Poppl, L., Toth, E., Toth, M., Paszli, I., Izvekov, V., Gabor, M. (1998). Synthesis and Characterizations of hydroxy-Aluminum cross-linked montmorillonite. *Journal of Thermal Analysis*, 53: 585-596.

[46] Carriazo, J.G., Moreno-Forero, M., Molina, R.,A., Moreno, S. (2010). Incorporation of titanium and titanium–iron species inside a smectite-type mineral for photocatalysis. *Applied Clay Science*, 50: 401-408.

[47] Kannan, S.K., Sundrarajan, M. (2015). Green synthesis of ruthenium oxide nanoparticles: Characterization and its antibacterial activity. *Advanced Powder Technology*, 26: 1505-1511.

[48] Jeng, J.S., Lin, Y.T., Chen, J.S. (2010) Preparation and characterization of transparent semiconductor RuO_2–SiO_2 films synthesized by sol–gel route. *Thin Solid Films*, 518: 5416-5420.

[49] Ismail, A.A., Bahnemann, D.W., Al-Sayari, S.A. (2012). Synthesis and photocatalytic properties of nanocrystalline Au, Pd and Ptphotodeposited onto mesoporous RuO_2-TiO_2nanocomposites. *Applied Catalysis A: General*, 431-432:,62-68.

[50] Hosokawa, S., Fujinami, Y., Kanai, H. (2005). Reactivity of Ru=O species in RuO_2/CeO_2 catalysts prepared by a wet reduction method. *Journal of Molecular Catalysis A: Chemical*, 240: 49-54.

[51] Corma, A. (1997). From Microporous to Mesoporous Molecular Sieve Materials and Their Use in Catalysis. *Chemical Reviews*, 97: 2373-2419.

[52] Chae, H.J., Nama, I.S., Ham, S., Bong Hong, S. (2001). Physicochemical characteristics of pillared interlayered clays. *Catalysis Today*, 68: 31-40.

[53] Guisnet, M., Ayrault, P., Coutanceau, C., Alvarez, M.F., Datkac, J. (1997). Acid properties of dealuminated beta zeolites studied by IR spectroscopy. *Journal of Chemical Society, Faraday Transactions*, 93: 1661-1665.

[54] Bineesh, K.V., Kim, S.Y., Jermy, B.R., Park, D.W. (2009). Synthesis, characterization and catalytic performance of vanadia-doped delaminated zirconia-pillared montmorillonite clay for the selective catalytic oxidation of hydrogen sulfide. *Journal of Molecular Catalysis A: Chemical*, 308: 150-158.

[55] Sorlino, M., Busca, G. (1984). FT-IR Study of the acid sites on the surface of silica supported ruthenium oxide. *Applications of Surface Science*, 18: 268-2672.

[56] Alotaibi, M.T., Taylor, M.J., Liu, D., Beaumont, S.K., Kyriakou, G. (2016). Selective oxidation of cyclohexene through gold functionalized silica monolith microreactors. *Surface Science*, 646: 179-185.

[57] Zhou, J., Cao, S., Yang, X., Chen, Q., Luo, X., Zheng, M. (2017). Highly selective allylic oxidation of cyclohexene over molybdenum-doped manganese oxide catalysts. *Reaction Kinetics, Mechanisms and Catalysis*, 120: 567–578.

[58] Qadir, M.I., Scholten, J.D., Dupont, J. (2014). TiO_2nanomaterials: Highly active catalysts for the oxidation of hydrocarbons. *Journal of Molecular Catalysis A: Chemical*, 383-384: 225-230.

[59] Corma, A., Garcıa, H. (2002). Lewis Acids as Catalysts in Oxidation Reactions: From Homogeneous to Heterogeneous Systems. *Chemical Reviews*, 102: 3837-3892.

[60] Ding, Z., Kloprogge, J.T., Frost, R.L., Lu, G.Q., Zhu, H.Y. (2001). Porous Clays and Pillared Clays-Based Catalysts. Part 2: A Review of the Catalytic and Molecular Sieve Applications. *Journal of Porous Materials*, 8: 273-293.

[61] Cai, X., Wang, H., Zhang, Q., Tong, J., Lei, Z. (2014). Magnetically recyclable core–shell Fe_3O_4@chitosan-Schiff base complexes as efficient catalysts for aerobic oxidation of cyclohexene under mild conditions. *Journal of Molecular Catalysis A: Chemical*, 383-384:217-224.

[62] Silva, F.P., Jacinto, M.J., Landers, R., Rossi, L.M. (2010). Selective Allylic oxidation of Cyclohexene by a Magnetically Recoverable Cobalt Oxide Catalyst. *Catalysis Letters*, 141: 432-437.

[63] Jorda, E., Tuel, A., Teissier, R., Kervennal, J. (1998). Synthesis, Characterization, and Activity in the Epoxidation of Cyclohexene with Aqueous H_2O_2 of Catalysts Prepared by Reaction of TiF_4 with Silica. *Journal of Catalysis*, 175: 93-107.

[64] Belaidi, N., Bedrane, S., Choukchou-Braham, A., Bachir, R. (2015). Novel vanadium-chromium-bentonite green catalysts for cyclohexene epoxidation. *Applied Clay Science*, 107: 14–20.

[65] Ghiaci, M., Aghabarari, B., Botelho do Rego, A.M., Ferraria, A.M., Habibollahi, S. (2011). Efficient allylic oxidation of cyclohexene catalyzed by trimetallic hybridnano-mixed oxide (Ru/Co/Ce). *Applied Catalysis A: General*, 393: 225-230.

[66] Kanmani, A.S., Vancheesan, S. (1998). Oxidation of cyclohexene and styrene catalysed by ruthenium(II) complexesunder homogeneous conditions. *Recent Advances in Basic and Applied Aspects of Industrial Catalysis Studies in Surface Science and Catalysis*, 113: 285-292.

[67] Azzi, H., Rekkab-Hammoumraoui, I., Chérif-Aouali, L., Choukchou-Braham, A. (2019). Mesoporous Co_3O_4 as a New Catalyst for AllylicOxidation of Cyclohexene. *Bulletin of Chemical Reaction Engineering & Catalysis*, 14 (1): 112-123.

[68] Canepa, A.L., Chanquia, C.M., Eimer, G.A., Casuscelli, S.G. (2013). Oxidation of olefins employing mesoporous molecular sieves modified with copper. *Applied Catalysis A: General*, 462– 463: 8– 14.

[69] Chanquia, C.M., Canepa, A.L., Bazan-Aguirre, J., Sapag, K., Rodriguez-Castellon, E., Reyes, P., Herrero, E.R., Casuscelli, S.G., Eimer, G.A. (2012). Copper-containing spherical mesoporous silicates prepared by template-ion exchange: A multitechnique characterization and oxidation properties. *Microporous and Mesoporous Materials,* 151: 2-12.

[70] Chanquia, C.M., Canepa, A.L., Winkler, E.L., Rodriguez-Castellon, E., Casuscelli, S.G., Eimer, G.A. (2016). Nature of active vanadium nanospecies in MCM-41 type catalysts for olefins oxidation. *Materials Chemistry and Physics,* 175: 172-179.